

**Enhanced distribution of NK012, a
polymeric micelle-encapsulated SN-38,
and sustained-release of SN-38 within
tumors can beat a hypovascular tumor**

先端生命科学専攻

がん先端生命科学分野

47-66524 齋藤 洋平

指導教員 松村 保広

Enhanced distribution of NK012, a polymeric micelle-encapsulated SN-38, and sustained-release of SN-38 within tumors can beat a hypovascular tumor

(NK012 の腫瘍内集積性と SN-38 の長期徐放能が血管の乏しい腫瘍に有効である)

2008 年 3 月修了

先端生命科学専攻 がん先端生命科学分野

学生証番号 47-66524 氏名 齋藤 洋平

指導教員名 松村 保広 准教授

キーワード DDS; NK012; micelle; SN-38; pancreatic cancer

Human pancreatic cancer is generally hypovascular in nature and rich in interstitium. These pathological barriers may be some of the factor that make human pancreatic cancer intractable, because they may hinder the penetration of anticancer agents throughout the pancreatic tumor tissue. Approximately 80% of the SN-38 inside NK012, a SN-38 incorporating micelles, can be gradually released within under physiological conditions. The aim of this study was to determine if NK012 may be an appropriate formulation for the treatment of hypovascular tumors. Among pancreatic tumor xenografts, PSN1 appeared to have the richest tumor vasculature and the least number of stromal cells and matrix. On the other hand, Capan1 had the poorest tumor vasculature and most abundant stromal tissue. Fluorescence microscopy and HPLC analysis demonstrated that while NK012 accumulated and continued to be distributed for more than 48 hs throughout the entire body of both tumors, CPT-11 disappeared almost entirely from both tumors within 6 hs. In addition, efficient sustained-release of SN-38 was maintained for more than 96 hs in both tumors following administration of NK012. On the other hand, following the administration of CPT-11, SN-38 was no longer detectable after 24 hs in the Capan1 tumor and after 48 hs in the PSN1 tumor. All tumors were eradicated in the mice treated with NK012 but not in those treated with

CPT-11. Since the antitumor activity of SN-38 is time-dependent, NK012, which combines enhanced distribution with sustained release of SN-38 within tumors may be ideal for the treatment of hypovascular tumors, such as pancreatic cancer.

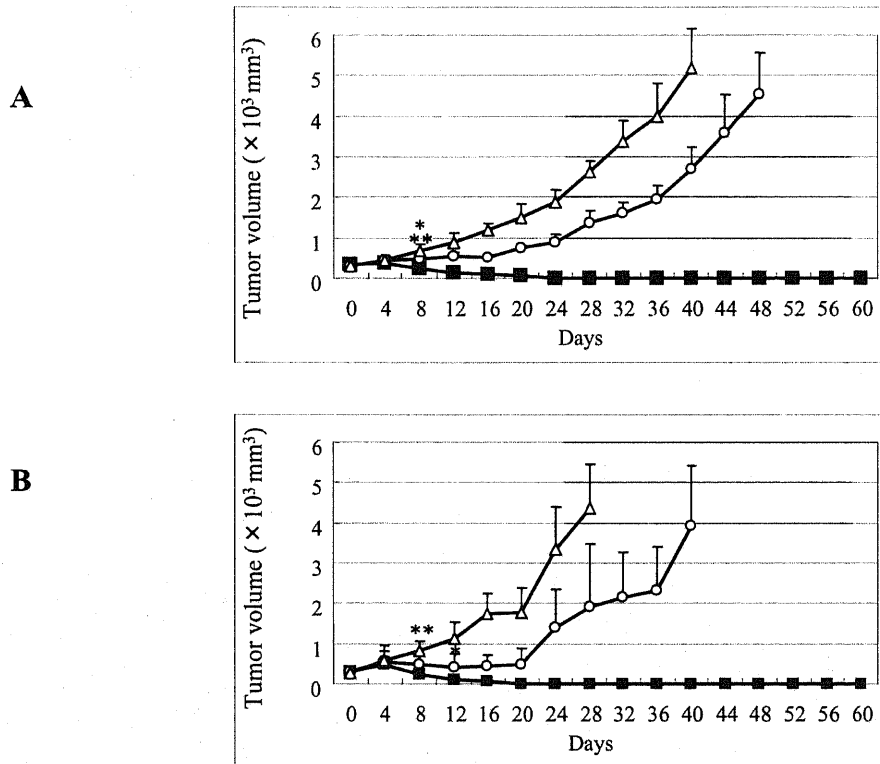


Figure. Anti tumor effect of NK012 and CPT-11.

NK012 (■), CPT-11 (○), or saline (△) was administered i.v. When the mean tumor volumes reached a 300 mm³ (on day 0), NK012 (30 mg/kg/d) or CPT-11 (66.7 mg/kg/d) was administered on days 0, 4, and 8. Each group consisted of 5 mice. A, Capan1 tumor; B, PSN-1 tumor. * $P < 0.05$ (NK012 vs CPT-11), ** $P < 0.05$ (NK012 vs saline)

Yohei Saito, Masahiro Yasunaga, Junichiro Kuroda, Yoshikatsu Koga, Yasuhiro Matsumura. Enhanced distribution of NK012 and sustained-release of SN-38 within tumors can beat a hypovascular tumor (*in press*, 2008)

Contents

1 Introduction

3 Materials and Methods

11 Results

15 Discussion

21 References

25 Figures

Introduction

Pancreatic cancer has one of the worst prognoses among cancers. ⁽¹⁾ The median survival of cases of advanced pancreatic cancer is only about half a year after systemic gemcitabine-based chemotherapy. ⁽²⁾ The recent success of molecular-targeting agents has also had some impact on pancreatic cancer treatment. A recent phase III trial of gemcitabine alone vs. gemcitabine plus erlotinib (a tyrosine kinase inhibitor) in patients with advanced pancreatic cancer revealed that the overall survival was significantly prolonged in the gemcitabine plus erlotinib arm. However, the median survival in the gemcitabine + erlotinib and gemcitabine alone arms was 6.24 months and 5.91 months, respectively, that is, only 10 days longer in the gemcitabine + erlotinib arm. ⁽³⁾ There is, therefore, an urgent need to develop modalities by which cytotoxic drugs can exert their significant antitumor activity to full potential and reasonably prolong the overall survival in patients with advanced pancreatic cancer. There may be several reasons why pancreatic cancer is intractable. It is conceivable that anticancer agents administered are not delivered efficiently enough to the pancreatic cancer cells to kill them. Pancreatic cancer tissue is generally hypovascular in nature ^(4, 5) and is rich in stromal cells and extracellular matrix, and these pathological barriers may hinder efficient penetration of the anticancer agents throughout the entire body of pancreatic cancer.

The role of drug delivery systems (DDS) is to selectively deliver cytotoxic drugs to tumor tissues while lessening their distribution to normal tissues in order to reduce their side effects. ⁽⁶⁻⁸⁾ However, it is conceivable that satisfactory drug delivery cannot be achieved in cancers having very few tumor vessels and an abundant collagen-rich interstitium. Therefore, a more sophisticated DDS may be needed for efficient delivery of drugs to such types of cancer as pancreatic cancer.

SN-38, a biologically active metabolite of irinotecan hydrochloride (CPT-11), has potent antitumor activity but has not been used clinically because of its water-insolubility. NK012, a drug formulation composed of SN-38-incorporating polymeric micelles, has been successfully developed recently, and the remarkable antitumor effects of NK012 against the human small cell lung cancer SBC-3, especially the VEGF-secreting SBC-3/VEGF tumor, has been demonstrated. ⁽⁸⁾

In the present study, we clarified the relationship between the tumor vasculature and tumor interstitium using several human pancreatic xenografts, and evaluated the therapeutic effect of NK012 in a hypovascular and hypervascular pancreatic tumor.

Materials and Methods

Drugs and Cells

SN-38 and NK012 were synthesized by Nippon Kayaku Co.,Ltd. (Tokyo, Japan). CPT-11 was purchased from Yakult Co.,Ltd. (Tokyo, Japan). The human pancreatic cancer cell lines, Panc1, PSN1, BxPC3 and Capan1, were purchased from American Type Culture Collection (Rockville, MD).

Panc1, PSN1 and Capan1 were maintained in DMEM supplemented with 10% fetal bovine serum, streptomycin, and L-glutamine (Sigma, St.Louis, MO) in atmosphere of 5% CO₂ at 37°C. BxPC3 were maintained in RPMI1640 supplemented with 10% fetal bovine serum, streptomycin and L-glutamine (Sigma, St.Louis, MO) in atmosphere of 5% CO₂ at 37°C.

Experimental mouse model

Female BALB/c nude mice, 6 weeks old, were purchased from CLEA Japan (Tokyo, Japan). Mice were inoculated subcutaneously (s.c.) in the flank with 1×10^7 cells/300 μ l PBS of each cell line. All animal procedures were performed in compliance with the guidelines for the care and use of experimental animals, laid down by the Committee for Animal Experimentation of the National Cancer Center; these guidelines meet the

ethical standards required by law and also comply with the guidelines for the use of experimental animals in Japan.

Immunohistochemical study of various human pancreatic tumor xenografts

When the tumor volume reached 300 mm³, tumors were excised from the mice and used for immunohistochemical analysis. To stain the blood vessel, the tissues were embedded in Optimal Cutting Temperature Compound (Sakura Finetechnochemical Co., Ltd., Tokyo, Japan) and frozen at -80°C until use. Six-micrometer-thick tumor sections were prepared using a cryostatic microtome, Tissue-Tek Cryo3 (Sakura Finetechnochemical Co., Ltd., Tokyo, Japan), and then air-dried for 1 h. The sections were soaked in 10% formalin for 15 min, and washed three times with 0.2 M phosphate-buffered saline (PBS). The sections were then rinsed with ultrapure water. Endogeneous peroxidase was blocked with a 0.3% hydrogen peroxide solution in 100% methanol for 20 min. The sections were then rinsed three times with PBS for 3min each. Nonspecific protein binding was blocked with 5% skim milk (BD, Franklin Lakes, NJ, USA) in PBS for 30 min at room temperature. After draining off the skim milk solution, polyclonal antibody against factor VIII (Zymed Laboratories Co., Ltd., South San Francisco, USA) was added at a dilution of 1:50, followed by incubation for 1 h and

three rinses with PBS for 5 min each. Biotinylated anti-rabbit IgG was added at a dilution of 1:50, followed by incubation for 1 h. The sections were rinsed three times with PBS, and VECTASTAIN Elite ABC Reagent (Vector Laboratories., Burlingame CA., USA) was added for 30 min. The sections were rinsed again three times with PBS and incubated with the 3, 3'-Diaminobenzidine Tetrahydrochloride (DAB+) Liquid System (Dako, Glostrup, Denmark) for 30 sec. Finally, the sections were rinsed and counterstained with hematoxylin solution. For staining for type I, III, and IV collagen, tissues were fixed with 4% formalin, and the paraffin sections were prepared by the Tokyo Histopathologic Laboratory Co., Ltd. (Tokyo, Japan). First, the sections were soaked three times for 5 min each in xylene, and then three times for 3 min each in ethanol for removing paraffin. The sections were then rinsed with ultrapure water and endogeneous peroxidase was blocked with a 0.3% hydrogen peroxide solution in 100% methanol for 20 min, followed by three rinses for 5 min with PBS. Then, Proteinase K (Dako Co., Glostrup, Denmark) was added. After the sections were rinsed three times for 5 min each with 0.2 M PBS, nonspecific protein binding was blocked with a 1% Normal Goat Serum (Dako Co., Glostrup, Denmark) solution in PBS for 30 min at room temperature. Then, after three rinses for 5 min each with PBS, polyclonal rabbit anti-type I, III, and IV collagen antibody (Dako, Glostrup, Denmark) was added at a dilution

of 1:500 (type I collagen), 1:10000 (type III collagen), and 1:2000 (type IV collagen), followed by incubation for 1 h. The slides were rinsed in PBS and incubated for 30 min with Envision/HRP (Dako, Glostrup, Denmark) directed against the primary antibody. After further rinsing, the sections were incubated with the DAB+ Liquid System (Dako, Glostrup, Denmark) for 30 sec. Then, after a final rinse, the sections were counterstained with hematoxylin solution.

***In vitro* growth assay**

The growth inhibitory effects of NK012, SN-38, and CPT11 were examined by the WST8 assay. Cell suspensions (5,000 cells/100 μ l) were seeded into a 96-well microliter plate, which was incubated for 24 hs at 37°C. Then, after removal of the medium, 100 μ L of medium containing various concentrations of each drug was added to the wells, which were then incubated for 48 hs at 37°C. Then, after removal of the medium, 10 μ l of WST8 solution and 90 μ l of medium was added to the wells, followed by incubation for 4 hs at 37°C. The growth inhibitory effect of each drug was assessed spectrophotometrically (SpectraMax 190, Molecular Devices Corp., Sunnyvale, CA).

Distribution studies of CPT-11 and NK012 in the tumors by fluorescence

microscopy

Nude mice bearing PSN1, as a hypervascular tumor model, or Capan1, as a hypovascular tumor model, were used for studying the distribution of NK012 and CPT-11, when the tumors reached 300 mm³ in volume. The MTD of NK012 (30 mg/kg) or CPT-11 (66.7 mg/kg) was injected i.v. into the mice. At 1, 6, 24, or 48 hs after the injection of NK012 or CPT-11, the mice were administered fluorescein labeled *Lycopersicon esculentum* lectin (100 µl/mouse) (Vector Laboratories, CA, USA) for the purpose of visualizing the tumor blood vessels. The tumors were then excised and embedded in optimal cutting temperature compound (Sakura Finetechnochemical Co., Ltd., Tokyo, Japan) and frozen at -80°C. Six-micrometer-thick tumor sections were then prepared using a cryostatic microtome, Tissue-Tek Cryo3 (Sakura Finetechnochemical Co., Ltd., Tokyo, Japan). The frozen sections were examined under a fluorescence microscope, BIOREVO (KEYENCE., Osaka., Japan) at an excitation wavelength of 377 nm and emission wavelength 447 nm in order to evaluate the distribution of CPT-11 and NK012 within the tumor tissues. Since formulations containing SN-38 bound via ester bonds possess a particular fluorescence, both CPT-11 and NK012 were detected under the same fluorescence conditions.

Distribution studies of free SN-38, CPT-11, and NK012 in the tumors by HPLC

When PSN1 and Capan1 tumors reached 300 mm³ in volume, NK012 (30 mg/kg) or CPT-11 (66.7 mg/kg) was administered i.v. to the mice. At 1, 6, 24, 72, or 96 hs after the injection of NK012 and CPT-11, each tumor was excised. The tumor tissues were rinsed with physiologic saline, mixed with 0.1 M glycine-HCl buffer (pH 3.0) / methanol at 5 w/w%, and homogenized. To detect free SN-38 and CPT-11, the tumor samples (100 µl) were mixed with 20 µl of 1mM phosphoric acid / methanol (1:1), 40 µl ultrapure water, and camptothecin (CPT) was used as the internal standard (10 ng/ml for free SN-38, 15 ng/ml for CPT-11). The samples were vortexed vigorously for 10 sec, and filtered through Ultrafree-MC Centrifugal Filter Devices (Millipore Co., Bedford, MA). Reversed-phase high-performance liquid chromatography was conducted at 35°C on a Mightysil RP-18 GP column 150 × 4.6 mm (Kanto Chemical Co., Inc., Tokyo, Japan). The samples were injected into an Alliance Water 2795 high-performance liquid chromatography system (Waters, Milford, MA) equipped with a Waters 2475 multi λ fluorescence detector. The detector was set at 365 and 430 nm (excitation and emission wavelengths, respectively) for CPT-11, and at 365 and 540 nm for SN-38.

For polymer-bound SN-38 detection, SN-38 was released from the conjugate as described previously. ⁽⁸⁾ In brief, 100 µl of tissue samples were diluted with 20 µl of

methanol (50 w/w%) and 20 µl of NaOH (0.7 M). The samples were incubated for 15 min at room temperature. After incubation, 20 µl of HCl (0.7 M) and 60 µl of internal standard solution was added to the samples, and then the hydrolysate was filtered. The filtrate was applied to the high-performance liquid chromatography system.

Polymer-bound SN-38 was determined by subtraction of non-polymer-bound SN-38 from the total SN-38 in the hydrolysate.

Antitumor activity of NK012 and CPT-11 against Capan1 or PSN1 xenografts

When the tumor volume reached approximately 300 mm³ in volume, the mice were randomly divided into test groups consisting of 5 mice per group (Day 0). The drugs were administered on Days 0, 4, and 8 by i.v. injection into the tail vein. NK012 was given at the dose of 30 mg/kg/d (maximum tolerated dose) and CPT-11 was given at the maximum tolerated dose of 66.7 mg/kg/d as indicated in the optimal schedule reported previously.⁽⁹⁾

The length (L) and width (W) of the tumor mass were measured every 3 days. The tumor volume (TV) was calculated as follows; $TV = (L \times W^2) \times 0.5233$.

Statistical analysis

Student's *t*-test was used for the statistical analyses. And $P < 0.05$ was considered to denote statistical significance.

Results

Density of collagen and the number of tumor blood vessels in the various human pancreatic tumor xenografts

We examined the density of collagen in four pancreatic cancer xenografts (Fig 1A). Type I collagen was present in the greatest abundance in Capan1 and least abundance in PSN1. The density of type I collagen in Panc1 and BxPC3 was in the second and third place, respectively.

Capan1 exhibited the highest in density of type III collagen, and BxPC3 and PSN1 were in the second and the fourth place, respectively, with respect to the density of type III collagen.

The distribution of type IV collagen tended to be similar to that of type I and III collagen.

We also examined the number of tumor blood vessels (Fig 1B). The PSN1 tumor possessed the largest number of blood vessels among the tumors. On the other hand, the Capan1 xenografts had the smallest number of tumor blood vessels.

We summarize the results on collagen density and blood vessel number obtained in our study for each pancreatic xenograft. Capan1 was the most collagen-rich tumor, and the density of collagen was the lowest in PSN1. On the other hand, tumor blood vessels

were most abundant in PSN1 and least abundant in Capan1. Therefore, we decided to use Capan1 as a hypovascular tumor model and PSN1 as a hypervascular tumor model.

***In vitro* cytotoxic effects of NK012, SN-38, and CPT-11 against Capan1 and PSN1 cell lines**

The IC₅₀ values of NK012 for the two cell lines, Capan1 (Fig 2A) and PSN1 (Fig 2B), ranged from 0.001 μ M to 0.1 μ M.

NK012 exhibited a remarkably higher cytotoxic effect against both the cell lines as compared with CPT-11. On the other hand, the cytotoxic effect of SN-38 was similar to that of NK012.

The IC₅₀ value of each drug against PSN1 was almost similar to that of Capan1.

Antitumor activity analysis of NK012 and CPT-11 using Capan1 and PSN1 bearing nude mice

The antitumor activity was observed in mice treated with NK012 at the dose of 30 mg/kg/d and CPT-11 at the dose of 66.7 mg/kg/d *in vivo* (Fig 3). While CPT-11 exerted significant antitumor effect as compared with that in the control group in mice bearing the Capan1 tumor, the tumor volume continued to increase consistently. On the other

hand, in the mice treated with NK012, the tumor volume started to shrink on Day 8, and the tumor disappeared completely by Day 28 in all the treated mice bearing the Capan1 tumor.

Different from the observations for the Capan1 tumor, mice bearing the PSN1 tumor treated with CPT-11 showed a slight reduction of the tumor volume from Day 4 to Day 12. However, after Day 12, the tumor volume began to increase again. On the other hand, the tumor disappeared completely in all the mice bearing the PSN1 tumor treated with NK012.

Distribution studies of CPT-11 and NK012 in the solid Capan1 and PSN1 tumors

With the purpose of evaluating drug distribution and accumulation over time, sections of the tumor treated with NK012 or CPT-11 were examined by fluorescence microscopy. Also, we examined the number of tumor blood vessels. In sections of the Capan1 tumor treated with CPT-11, maximum drug accumulation was observed within 1h of the injection of CPT-11(Fig 4A). At 6 hs after the injection, the fluorescence originating from CPT-11 had almost entirely disappeared. Subsequently, no accumulation of CPT-11 was observed within the tumor tissues. On the other hand, in sections of the Capan1 tumor treated with NK012, fluorescence from NK012 began to

appear around tumor blood vessels at 1 h after the i.v. injection and lasted until 48 hs. After 6 hs, the fluorescence area began to increase and the maximum fluorescence area was observed at 24 hs after the injection. Similar results were obtained for the PSN1 tumor (Fig 4B).

These microscopic observations were confirmed quantitatively by measuring the amount of SN-38 that could be extracted from each of the solid tumors by reversed-phase HPLC. Only slight conversion to SN-38 from CPT-11 was seen from 1 h to 24 hs in the Capan1 tumor and from 1 h to 48 hs in the PSN1 tumor, and no SN-38 was seen detected thereafter. On the other hand, SN-38 released from NK012 continued to be detected in both tumors from 1 h to 96 hs after the injection of NK012 (Fig 5).

Discussion

Recently, several new formulations categorized as DDS have been approved in the field of oncological treatment, such as DoxilTM, a polyethylene glycol-liposome incorporated adriamycin^(10, 11) and abraxane, a taxol coated with albumin.^(12, 13) In addition, several clinical trials of drug based on DDS concept, are now underway.^(14- 16) Since such formulations possess a longer plasma AUC, liposomal drugs should have sufficient time to exit from tumor blood vessel and accumulate at reasonably high dose levels in the surrounding interstitium.

However, it was reported that although PEG-liposomes can be delivered efficiently to a solid tumor, free drug was not transferred sufficiently to cancer cells, particularly distant from the tumor vessels, because the formulations were too large to scamper about in the tumor interstitium.⁽¹⁷⁾ Also, it has been suggested that liposomes are too stable to allow the drug within to be released easily. Therefore, it has been speculated that PEG-liposomes may not be so effective against cancers in which the tumor vessel network is irregular and loose because of an abundant collagen-rich matrix. Some examples of such cancers include scirrhus cancer of the stomach and pancreatic cancer. In fact, DoxilTM is known to be effective clinically against ovarian cancer and breast cancer, both of which are characterized by a high density of tumor microvessels,

whereas it is not effective against stomach cancer and pancreatic cancer.⁽¹⁸⁾ Therefore, it is conceivable that some special device is necessary for DDS drugs to exert their antitumor effect sufficiently even against hypovascular tumors, such as pancreatic cancer.

In the present study, we characterized the tumor vessel and its interstitium using four kinds of human pancreatic xenografts. The results revealed that the number of tumor blood vessels was inversely related to the amount of collagen within the tumor tissues. Among the four cell lines, Capan1 was the poorest in tumor vasculature and richest in the amount of collagen within the tumor tissue. Conversely, PSN1 was the richest in tumor vasculature and poorest in the amount of collagen. Therefore, it may safely be said that Capan1 xenografts come the nearest to human pancreatic cancer tissue in terms of the amount of interstitial tissue among the four cell lines tested.

Then, we evaluated the *in vitro* cytotoxic effect of CPT-11, SN-38, and NK012 and the *in vivo* antitumor activity of CPT-11 and NK012 against Capan1 tumors, as a hypovascular tumor model and PSN1 tumors, as a hypervascular tumor model. SN-38 and NK012 exhibited a higher cytotoxic effect against the two cell lines as compared to CPT-11. Between SN-38 and NK012, the cytotoxic effect of NK012 was almost similar or a little lower as compared with that of SN-38. Since CPT-11 itself is a prodrug and is

converted to SN-38, an active metabolite of CPT-11, by carboxylesterases, the activity of CPT-11 is dependent on the activity of the enzymes. It is speculated that the efficient sustained release of SN-38 from NK012 allows the formulation to exert a similar cytotoxic effect to that of SN-38. In the *in vivo* experiment, CPT-11 showed significant antitumor activity against both PSN1 tumors as a hypervascular tumor model and Capan1 tumors as a hypovascular tumor model. A slight reduction of tumor size was observed from Day 4 to Day 12 in the case of PSN1 tumors, but not the Capan1 tumors. We suggested that the higher antitumor activity seen in PSN1 than Capan1 tumors is probably because of the great accumulation of CPT-11 in the PSN1 xenografts than in the Capan1 xenografts because of the more abundant vasculature in the former. Surprisingly, NK012 could cause complete disappearance of both PSN1 and Capan1 tumor xenografts. Before conducting the experiment, we had anticipated that NK012 might exert stronger antitumor effect against PSN1 as compared with that against Capan1, because such macromolecular drugs can accumulate more efficiently in the PSN1 xenografts because of the richer vasculature. Therefore, we then intensively examined the distribution of NK012 and CPT-11 within the PSN1 or Capan1 xenografts by fluorescence microscopy and HPLC. In the analysis by fluorescence microscopy, NK012 appeared within and around the tumor blood vessels in both the PSN1 and

Capan1 xenografts at 1h after the injection. NK012 began to spread from the blood vessel within the tumor tissue of both xenografts. Fluorescence originating from NK012 increased to the maximum in both the tumors by 24 hs after the injection of NK012. Namely, NK012 was distributed throughout the entire body of both the tumors at 24 hs after the injection. Furthermore, fluorescence originating from NK012 was clearly and diffusely detected throughout both the tumors.

On the other hand, fluorescence originating from CPT-11 increased to the maximum at 1 h in both tumors after the injection of CPT-11, indicating that maximum distribution of CPT-11 was achieved in both tumors within 1h of the injection. No or very slight fluorescence of CPT-11 was observed in both tumors at 6 hs after the injection of CPT-11. These observations were confirmed quantitatively by measuring the amount of SN-38 extracted from both tumors by reverse-phase HPLC. Only slight conversion to SN-38 from CPT-11 was seen from 1 h to 24 hs in the Capan1 tumor and from 1 h to 48 hs in the PSN1 tumor, and no SN-38 was detected thereafter. On the other hand, SN-38 released from NK012 continued to be detected in both tumors from 1 to 96 hs after the injection of NK012. In both CPT-11 and NK012, SN-38 binds to each counter molecule via an ester bond, which confers blue fluorescence on CPT-11 and NK012. Therefore, it is speculated that polymer bound SN-38 can be distributed throughout the entire body of

the tumor, regardless of the amount of interstitial tissue. We are unable to explain clearly how NK012 was distributed well even in hypovascular tumors. However, it is speculated that NK012 can move smoothly within the tumor interstitial because of the relatively small particle size (20 nm) as compared with that of other DDS formulations, and because of its flexibility, the formulation can pass through even narrow gaps within the interstitium. Previously, we reported that sustained release of 74% of free SN-38 occurred from NK012 under physiological conditions within 48 hs. ⁽⁸⁾ It is also important to remember that the antitumor activity of SN-38 is time-dependent. ⁽¹⁹⁾ Taking all of these data together, it may be concluded that NK012 can selectively accumulate in pancreatic tumor xenografts, to be distributed effectively throughout the entire body of the tumor, including in hypovascular tumors, and show sustained-release for a prolonged period of time. Consequently, NK012 can exert more significant antitumor activity as compared to CPT-11, which is not an ideal formulation for realizing the time-dependent actions of the drug.

In addition to our present study, there have been several efforts to enhance the accumulation of anticancer agents in tumors to obtain higher antitumor activities of drugs. For example, it has been reported that a TGF- β inhibitor could enhance the tumor vascular permeability to promote accumulation of macromolecules. ⁽²⁰⁾ Conversely,

combined use of an antiangiogenic agent, such as an antibody to VEGF, with an anticancer agent could enhance the antitumor activity, probably by lowering the tumor vascular permeability with consequent decrease of the interstitial fluid pressure so that the anticancer agents may accumulate more easily in the tumor.^(21, 22) However, much yet remains to be clarified.

In this paper, we have shown not only the superiority antitumor effect of NK012 as compared with that of CPT-11, but would also like to propose that enhanced accumulation, distribution, and retention of DDS within the tumor tissue and the sustained release of anticancer agents from DDS particles are key elements for the treatment of hypovascular tumors. A phase I clinical trial is now underway. Not only the clinical usefulness of NK012, but also the new concept for antitumor actions described in this paper are intended to be verified in the near future through further preclinical and clinical studies.

References

1. Jemal A, Siegel R, Ward E, Murray T, Xu J, Thun MJ. Cancer statistics, 2007. *CA Cancer J Clin* 2007; 57: 43-66.
2. Burris HA 3rd, Moore MJ, Andersen J, et al. Improvements in survival and clinical benefit with gemcitabine as first-line therapy for patients with advanced pancreas cancer: a randomized trial. *J Clin Oncol* 1997; 15: 2403-13.
3. Moore MJ, Goldstein D, Hamm J, et al. Erlotinib plus gemcitabine compared with gemcitabine alone in patients with advanced pancreatic cancer: a phase III trial of the National Cancer Institute of Canada Clinical Trials Group. *J Clin Oncol* 2007; 25: 1960-6.
4. Hosoki T. Dynamic CT of pancreatic tumors. *AJR Am J Roentgenol*. 1983; 140: 959-65.
5. Sofuni A, Iijima H, Moriyasu F, et al. Differential diagnosis of pancreatic tumors using ultrasound contrast imaging. *J Gastroenterol* 2005; 40:518-25
6. Matsumura Y, Maeda H. A new concept for macromolecular therapeutics in cancer chemotherapy: mechanism of tumoritropic accumulation of proteins and the antitumor agent smancs. *Cancer res* 1986; 46: 6387-92.
7. Muggia FM. Doxorubicin-polymer conjugates: further demonstration of the concept

of enhanced permeability and retention. *Clin Cancer Res* 1999; 5: 7-8.

8. Koizumi F, Kitagawa M, Negishi T, et al. Novel SN-38-incorporating polymeric micelles, NK012, eradicate vascular endothelial growth factor-secreting bulky tumors. *Cancer Res* 2006; 66: 10048-56.

9. Kawato Y, Furuta T, Aonuma M, Yasuoka M, Yokokura T, Matsumoto K. Antitumor activity of a camptothecin derivative, CPT-11, against human tumor xenografts in nude mice. *Cancer Chemother Pharmacol* 1991; 28: 192-8.

10. Muggia FM. Liposomal encapsulated anthracyclines: new therapeutic horizons. *Curr Oncol Rep* 2001; 3: 156-62.

11. Ferrari M. Cancer nanotechnology: opportunities and challenges. *Nat Rev Cancer* 2005; 5: 161-71.

12. Green MR, Manikhas GM, Orlov S, et al. Abraxane, a novel Cremophor-free, albumin-bound particle form of paclitaxel for the treatment of advanced non-small-cell lung cancer. *Ann Oncol* 2006; 17: 1263-8.

13. Gradishar WJ, Tjulandin S, Davidson N, et al. Phase III trial of nanoparticle albumin-bound paclitaxel compared with polyethylated castor oil-based paclitaxel in women with breast cancer. *J Clin Oncol* 2005; 23: 7794-803.

14. Matsumura Y, Hamaguchi T, Ura T, et al. Phase I clinical trial and pharmacokinetic

evaluation of NK911, a micelle-encapsulated doxorubicin. *Br J Cancer* 2004; 91: 1775-81.

15. Hamaguchi T, Matsumura Y, Suzuki M, et al. NK105, a paclitaxel-incorporating micellar nanoparticle formulation, can extend in vivo antitumour activity and reduce the neurotoxicity of paclitaxel. *Br J Cancer* 2005; 92: 1240-6.

16. Uchino H, Matsumura Y, Negishi T, et al. Cisplatin-incorporating polymeric micelles (NC-6004) can reduce nephrotoxicity and neurotoxicity of cisplatin in rats. *Br J Cancer* 2005; 93: 678-87.

17. Unezaki S, Maruyama K, Hosoda J, et al. Direct measurement of the extravasation of polyethylene glycol-coated liposomes into solid tumour tissue by in vivo fluorescence microscopy. *Int J Pharmacol* 1996; 144: 11-17.

18. Tsukioka Y, Matsumura Y, Hamaguchi T, Koike H, Moriyasu F, Kakizoe T. Pharmaceutical and biomedical differences between micellar doxorubicin (NK911) and liposomal doxorubicin (Doxil). *Jpn J Cancer Res* 2002; 93: 1145-53.

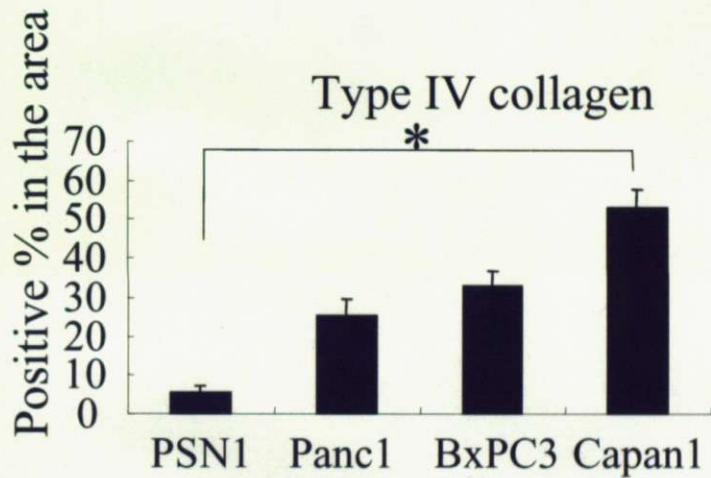
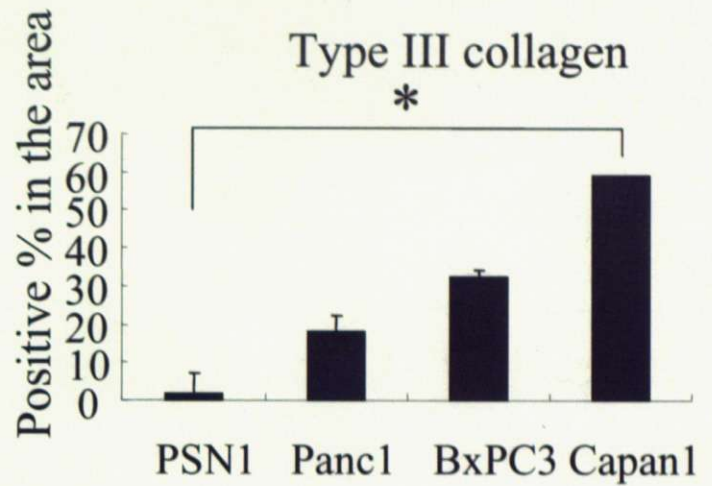
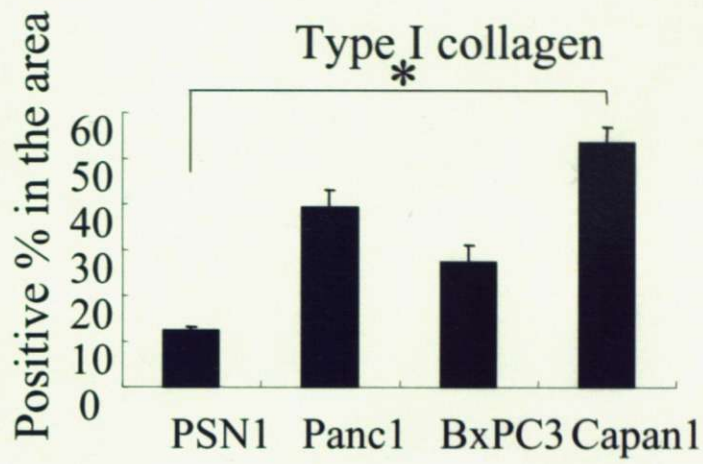
19. Kawato Y, Aonuma M, Hirota Y, Kuga H, Sato K. Intracellular roles of SN-38, a metabolite of the camptothecin derivative CPT-11, in the antitumor effect of CPT-11. *Cancer Res* 1991; 51: 4187-91.

20. Kano MR, Bae Y, Iwata C, et al. Improvement of cancer-targeting therapy, using

nanocarriers for intractable solid tumors by inhibition of TGF-beta signaling. Proc Natl Acad Sci U S A 2007; 104: 3460-5.

21. Jain RK. Normalizing tumor vasculature with anti-angiogenic therapy: a new paradigm for combination therapy. Nat Med 2001; 7: 987-9.

22. Jain RK. Normalization of tumor vasculature: an emerging concept in antiangiogenic therapy. Science 2005; 307: 58-62.



* P<0.001

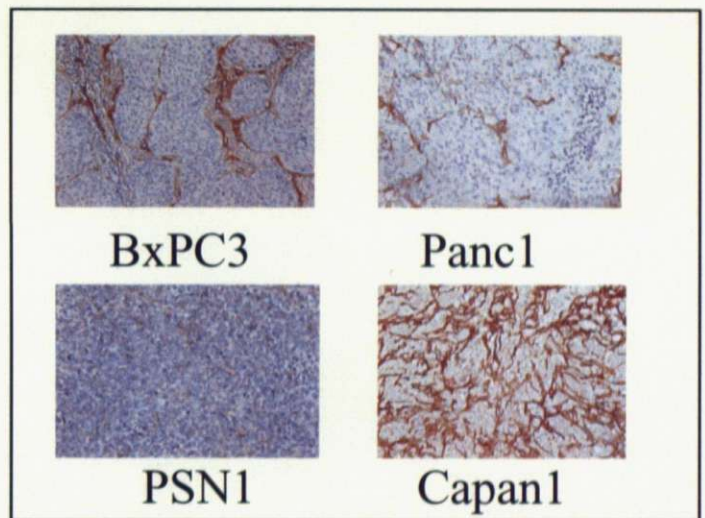
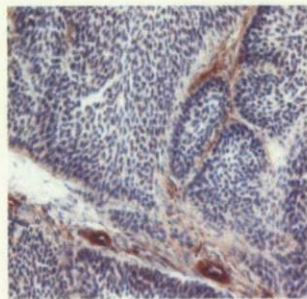
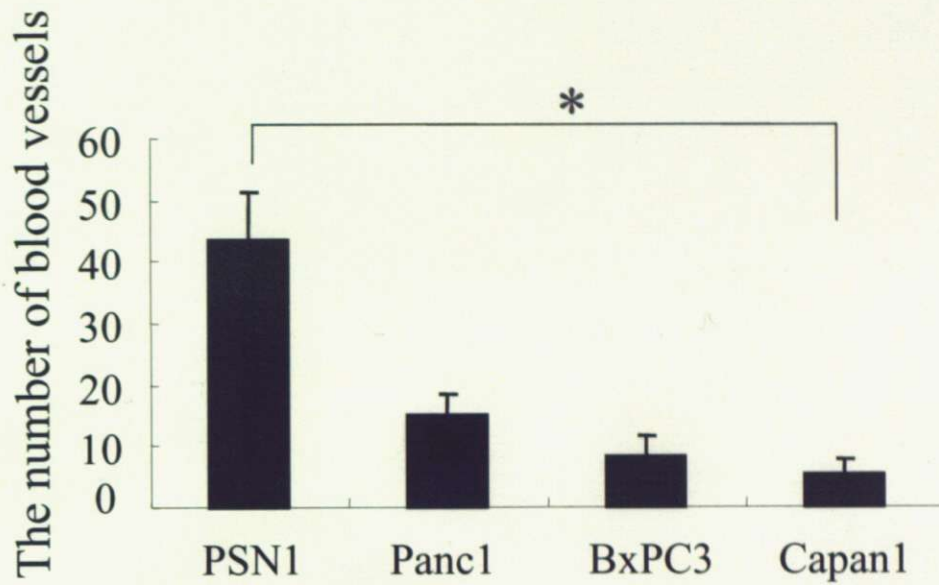
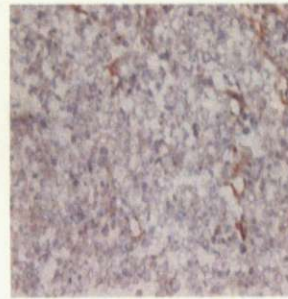


Figure 1A. Examination of the amount of stroma in four human pancreatic cancer xenografts.

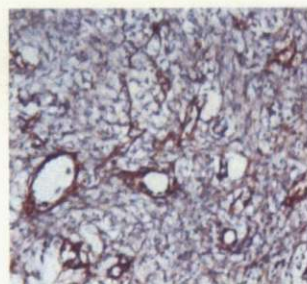
The amount of stroma in the four xenografts, BxPC3, Panc1, PSN1 and Capan1. Immunohistochemical staining was conducted in order to determine the distribution of type I, III and IV collagen in the tumors. The area occupied by each of type I collagen (left, upper), type III collagen (right, upper), and type IV collagen (left, bottom) was quantified. A representative immunostained image for type IV collagen is shown (right, bottom). *, P<0.05. bar, SD.



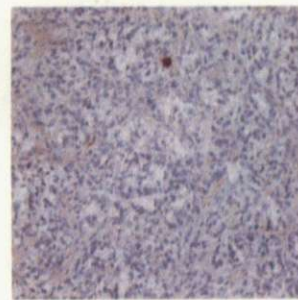
BxPC3



Panc1



PSN1



Capan1

Figure 1B. Examination of the number of tumor blood vessels in four human pancreatic cancer xenografts.

The number of blood vessels in the four xenografts. After immunostaining with anti factor VIII antibody, the number of tumor blood vessels in each of the xenograft was counted. *, $P < 0.05$. bar, SD.

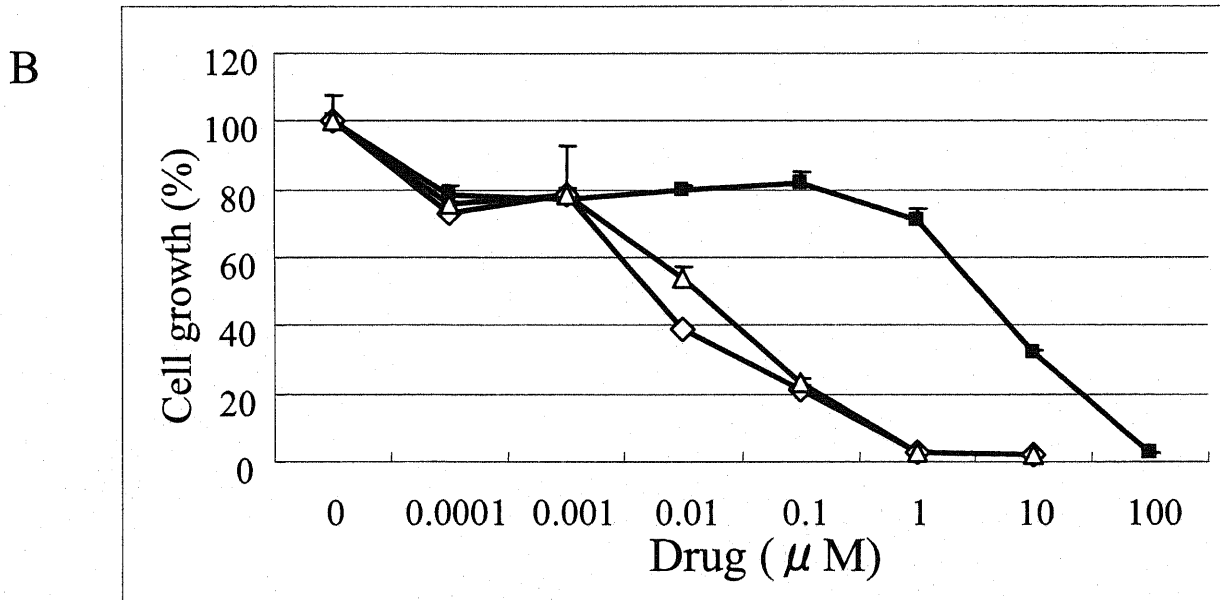
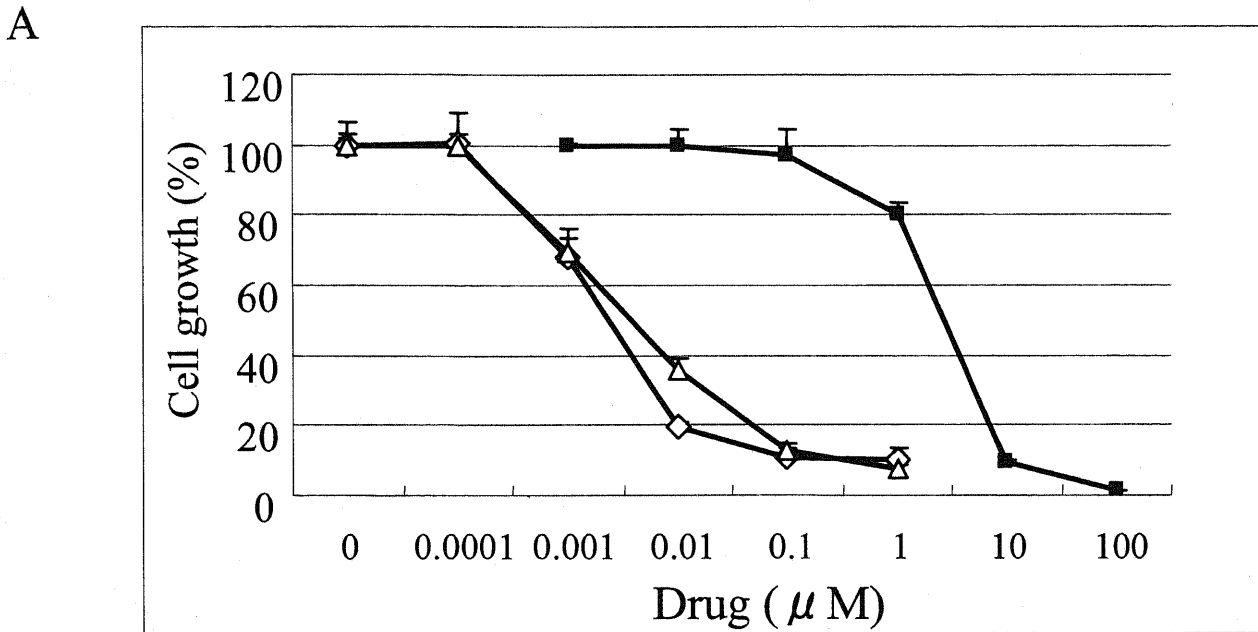
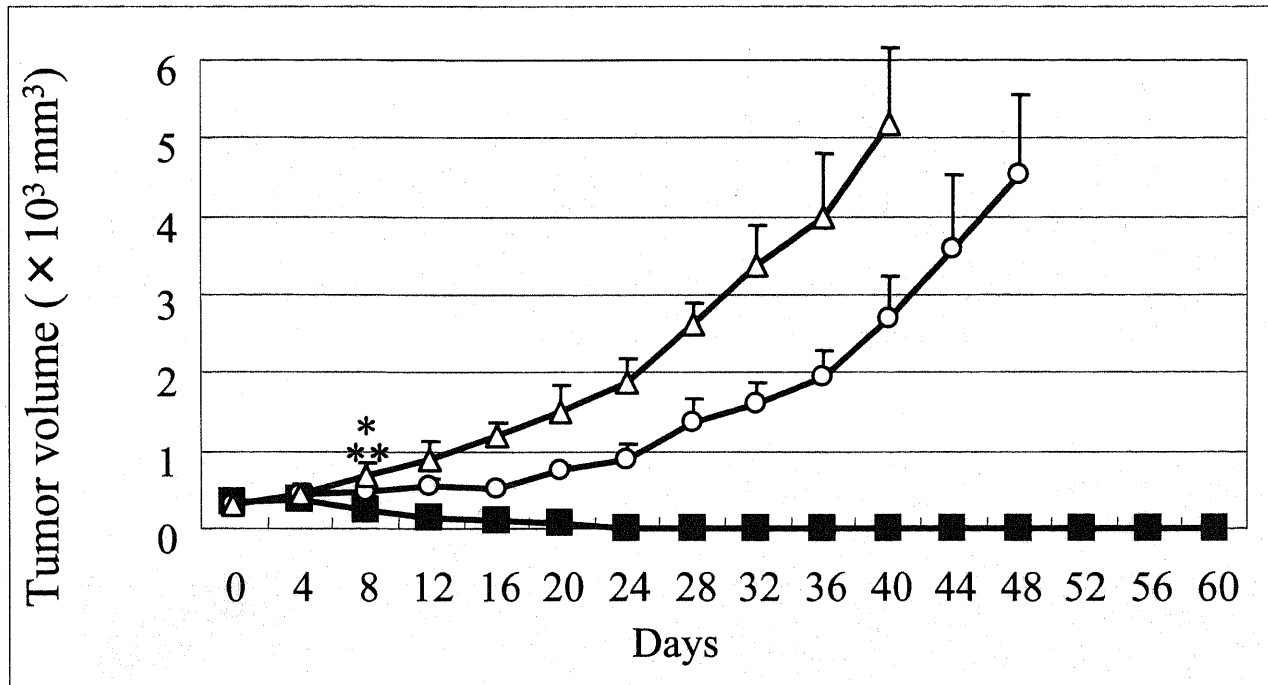


Figure 2. Capan1 cells (A) and PSN1 cells (B) were exposed to the indicated concentrations of each drug for 72 hs.

The growth inhibition curves for NK012 (Δ), SN-38 (\diamond), and CPT-11 (\blacksquare) are shown.

A



B

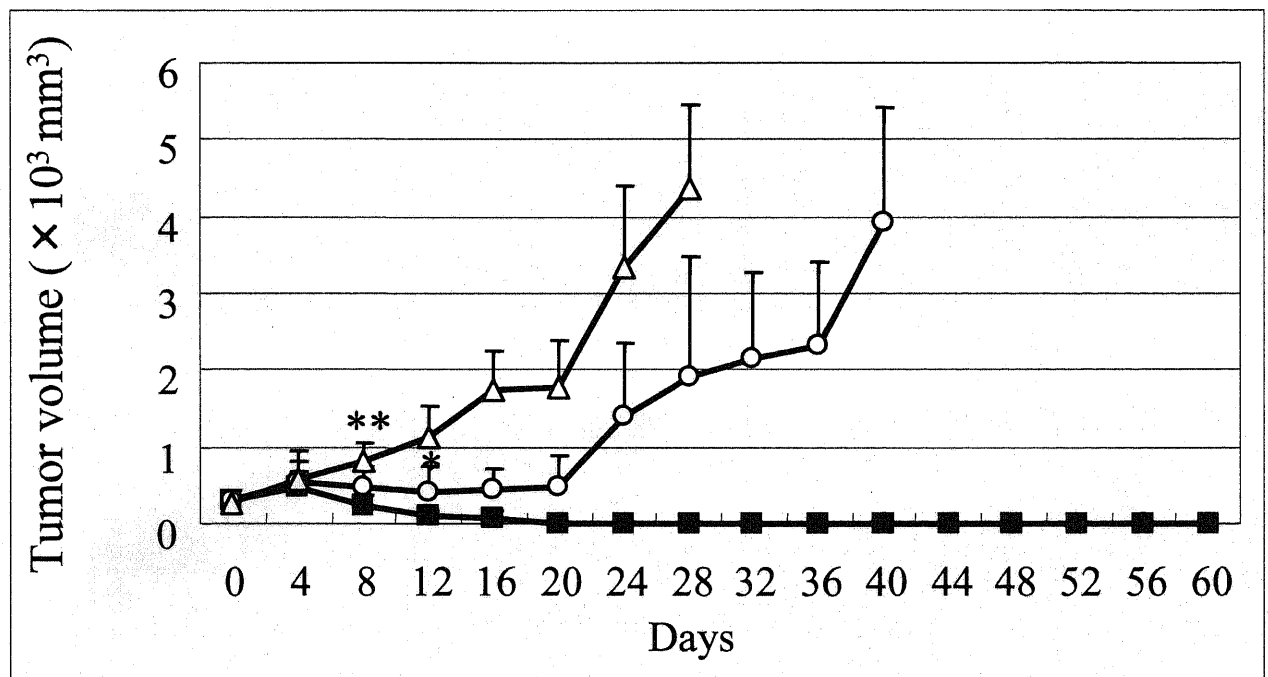


Figure 3. Anti tumor effect of NK012 and CPT-11.

NK012 (■), CPT-11 (○), or saline (△) was administered i.v. When the mean tumor volumes reached a 300 mm³ (on Day 0), NK012 (30 mg/kg/d) or CPT-11 (66.7 mg/kg/d) was administered on Day 0, 4, and 8. Each group consisted of 5 mice.

A, Capan1 tumor; B, PSN1 tumor *, $P < 0.05$ (NK012 vs CPT11)

** , $P < 0.05$ (NK012 vs saline)

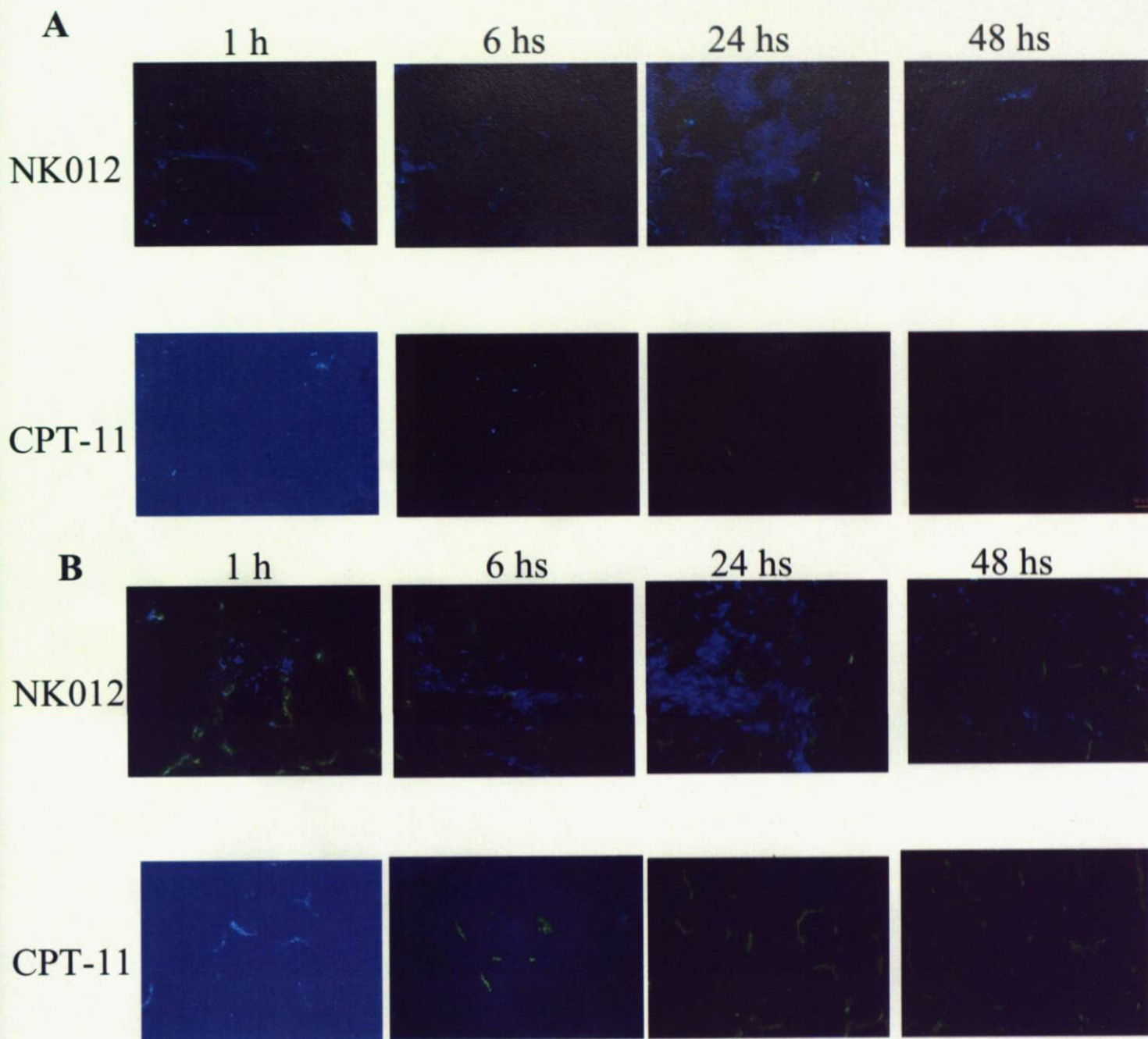


Figure 4. Distribution of NK012 or CPT-11 in the Capan1 (A) and PSN1 (B) tumor xenografts.

Mice bearing Capan1 or PSN1 tumors were injected with NK012 (30 mg/kg/d) or CPT-11 (66.7 mg/kg/d).

The tumor tissues were excised at 1, 6, 24, and 48 hs after the i.v. injection of NK012 or CPT-11. Each mouse was administered an injection of fluorescein labeled *Lycopersicon esculentum* lectin just before being sacrificed, for detecting the tumor blood vessels. The frozen sections were examined under a fluorescence microscope at an excitation wavelength of 377 nm and emission wavelength of 447 nm.

The same fluorescence condition can be applied for visualizing NK012 and CPT-11 fluorescence. Free SN-38 can not be detected under this fluorescence condition.

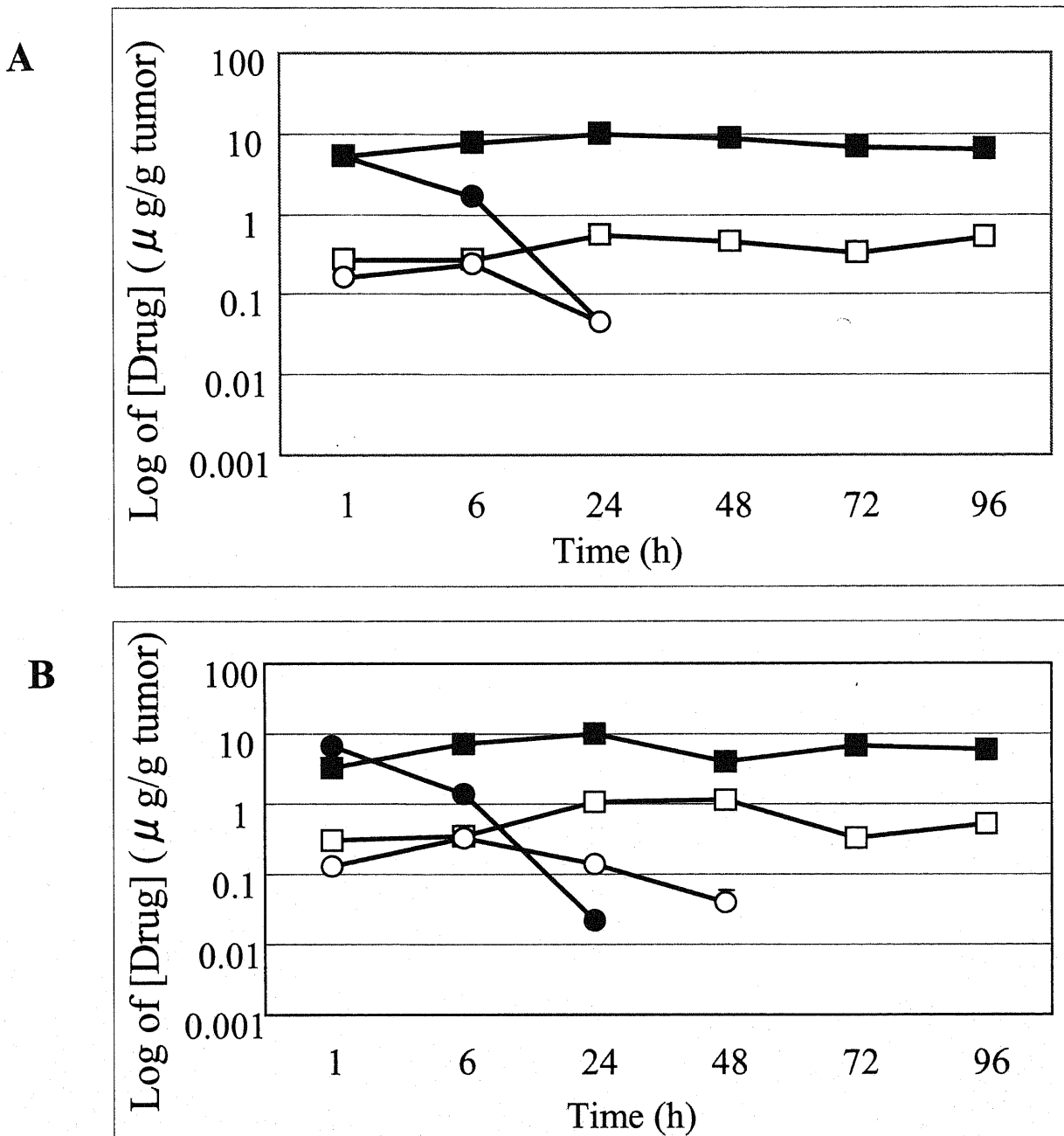


Figure 5. Tumor distribution of CPT-11, NK012 (or polymer bound SN-38), and free SN-38 after administration of NK012 and CPT-11 to mice bearing Capan1 (A) or PSN1 (B) xenografts.

The time profiles of polymer bound SN-38 (■), free SN-38 released from NK012 (□), CPT-11 (●), and free SN-38 converted from CPT-11 (○) were obtained by HPLC analysis. The time-points examined were 1, 6, 24, 48, 72, and 96 hs after the administration of CPT-11 or NK012.